Appendix

Supplemental information

The translational regulator FMRP controls lipid and glucose metabolism in mice and humans

Antoine Leboucher, Didier F. Pisani, Laura Martinez-Gili, Julien Chilloux, Patricia Bermudez-Martin, Anke Van Dijck, Tariq Ganief, Boris Macek, Jérôme A. J. Becker, Julie Le Merrer, Frank R. Kooy, Ez-Zoubir Amri, Edouard W. Khandjian, Marc-Emmanuel Dumas, Laetitia Davidovic

This PDF file includes:

Supplemental materials and methods

Figures S1 to S8

Tables S1 to S9 legends

Other supplemental materials for this manuscript include the following:

Tables S1 to S9, available as Excel files

Supplemental material and methods

Animal procedures. C57Bl6/J *Fmr1*-KO2 mice used in this study are described in [1]. Animals were housed in an SPF facility in medium-size (up to 5 animals/cage) or large cages (up to 10 animals/cage) filled with wooden bedding, one plastic house and nesting material for enrichment. All *Fmr1*-WT and *Fmr1*-KO male used in this study were littermates born to heterozygous females. Pups were weaned at 28 days of age, identified by ear tags, and genotyped by PCR as described [1]. Pups from various litters were then randomly grouped according to their genotype in cages and had *ad libitum* access to water and standard chow (reference 4RF25, Mucedola) composed of cereals (53.7%), animal proteins (4.7%), vegetal proteins (30.5%), lipids (soy oil, 1.4%), vitamins and minerals (4.1%), amino acids (0.1%). Animals were housed in a temperature (22-24°C) and hygrometry (70-80%)- controlled room with a 12 hrs light-dark cycle (lights on at 07:00). All the described experiments were performed on male animals at exactly 4-months (16 weeks) of age, to the exception of initial blood sampling of fed animals for metabolic profiling presented in Figure 1 that was performed on fed *Fmr1*-KO and WT animals between 4 and 6 months of age. Blood was withdrawn in the morning between 9 and 10 a.m. in heparinated tubes (Terumo) from *Fmr1-KO* and WT animals in nonfasting or fasting conditions as stated. In nonfasting conditions, animals were fed *ad libitum* and in fasting conditions animals were fasted overnight for 16 hr. Plasma was collected from tubes after

centrifugation at 1200g for 10 min. For experiments involving treatment, animals from the same genotype were randomly assigned to experimental groups.

Metabolic profiling. NMR experiments were carried out using a Bruker Avance spectrometer (Bruker GmbH, Rheinstetten, Germany) operating at 600 MHz. Briefly, 15 µL of plasma or serum was mixed with 335 µL of water and 350 µL of buffer (0.075M NaH_2PO_4, 0.8% TSP, 0.04% NaN_3, 20% D_2O, pH 7.4), centrifuged (12000g, 4 °C, 5 min). Six hundred µL of the resulting supernatant was transferred into a SampleJet NMR tube for ^1H NMR analysis using a spectrometer (Bruker) operating at 600.22 MHz as described previously [2]. Structural assignment was performed using data from literature, HMDB (http://www.hmdb.ca/), S-Base (Bruker GmbH, Rheinstetten, Germany) and in-house databases [3]. ^1H NMR spectra were pre-processed and exported in to Matlab for multivariate statistical analyses using orthogonal partial least square discriminant analysis (O-PLS-DA) as previously reported [4].

Blood chemistry and hormones measurements. The determination of circulating TG, FFA and total cholesterol was subcontracted to the Genotoul Anexplo Platform (Toulouse, France) and performed on 16 hr fasted *Fmr1*-WT and KO plasma samples. The determination of triglyceride content in liver was made using an enzymatic test (ETGA-200, Bioassay Systems) on tissue homogenates from 16 hr fasted animals. Briefly, tissues of *Fmr1* WT and KO mice were homogenized in proportion to their mass using a water-based buffer containing

isopropanol and Triton X100. The resulting homogenate was then centrifuged and the supernatant submitted to enzymatic hydrolysis of TG, followed by a chemical determination of glycerol, proportional to the amount of TG in the original sample, using a biochemical colorimetric kit (Sigma Aldrich). Leptin and insulin were measured on murine plasma sampled after a 16 hr fast using an Electro-Chemo-Luminescence (ECL)-based assay (v-plex®, MesoScaleDiscovery). The same platform was used to measure insulin in sera from FXS patients and controls.

Insulin (ITT), glucose tolerance tests (GTT). These experiments were conducted according to the IMPReSS guidelines (International Mouse Phenotyping Resource of Standardized Screens) and in agreement with [5] and [6]. Mice were respectively fasted 16 hr (GTT) or 6 hr (ITT) prior to i.p. injection of glucose (2 g/Kg, Sigma-Aldrich) or insulin (0.75 U/Kg, Humalog, Lilly) as per recommended procedures [6]. Glycemia was then measured by tail blood sampling at 0, 15, 30, 60, 90, 120 and 180 min post injection using a glucometer (AccuCheck Mobile, Roche) and a drop of blood collected after an incision at the tip of the tail. During the course of the experiment, mice were freely moving and unrestrained (including during blood sampling for glycemia measure) and had continuous access to water.

In vivo tissue insulin sensitivity measurement. Mice were fasted 16 hours, then injected with insulin (0.75 U/Kg, Humalog, Lilly) or saline. Five minutes after

injection, mice were sacrificed by cervical dislocation and tissues were rapidly dissected, snapped frozen in liquid nitrogen and stored at -80°C until further analyses.

Western-blotting. Samples were homogenized by sonication in a buffer containing 50 mM Tris pH 7.4, NaCl 150 mM, $MgCl_2$ 1.25 mM, Triton 0.5 % and containing protease and phosphatase inhibitors (Pierce, Thermo-Scientific). 17,000 g supernatants were dosed using the Bradford method (Biorad). 30 µg of proteins were diluted in Laemmli buffer, separated on 11% acrylamide gels and transferred to nitrocellulose membranes (Amersham). Membranes were probed with Anti-Akt (#9272; 1:2000), anti-pSer^{473}-Akt (#9271; 1:500), anti-Insulin receptor (#3025; 1:1000), anti-pTyr$^{1150/1151}$-Insulin receptor/pTyr$^{1135-1136}$Igf receptor (#3024; 1:250) polyclonal antibodies from Cell Signalling Technologies, monoclonal anti-β-Actin (#A2228) or anti-GAPDH (#G8795) antibodies (1:30,000; Sigma-Aldrich) and HRP-coupled secondary antibodies (1:1000; Jackson Laboratories). Signal was visualized using ECL kits (Perkin) and a Fusion VX-Imager (Vilber). Protein and phospho-proteins signals were quantified by densitometric analysis using the ImageJ software. For each tissue, two gels were run in parallel. One membrane was used for total proteins quantification and the other for phosphoproteins. β-actin signals were used to control for variability in loading/transfer. Total protein and phospho-protein signal intensities were normalized to the respective β-actin signals. The ratio between normalized phospho-epitopes signals and the corresponding normalized total protein signal

was then calculated. Scans of the fully uncut Ponceau-stained membranes as well as western-blots are available upon request.

Quantitative RT-PCR. Total RNA was extracted from tissues using the RNeasy kit (Qiagen, Hilden, Germany) and digested with DNAase I (Turbo DNAse, Ambion). Reverse transcription (RT) reaction was performed using the Superscript II RT-PCR system (Invitrogen, Carlsbad, California, USA) according to the manufacturers' protocol. Real-time PCR reactions were carried out using the Syber Green I qPCR core Kit (Eurogentec, Liège, Belgium) in a LightCycler system (Roche, USA). The comparative threshold cycle (C_t) for the amplicons of each sample was determined by the LightCycler software and normalised to the corresponding C_t of *TATA Box Binding Protein* (*Tbp*) mRNA for murine samples and *Glyceraldhyde phosphate dehydrogenase* (*GAPDH*) for human samples. Finally, the $2^{-\Delta\Delta C_t}$ method [7] was used to analyse the relative changes in the various studied mRNAs. The following primers were used: *Tbp* (AGGCCAGACCCCACAACTC; GGGTGGTGCCTGGCAA), *Pdgfra* (ACTACATCTCCAAAGGCAGCACCT, TGTAGAACTGGTCGTTCATGGGC A), human *GAPDH* (CCACATCGCTCAGACACCAT; GACCAGGCGCCCAAT), human *FMR1* (CATGCACTTTCGGAGTCTG; GAAATCTCGAGGCAAGCTG). Primers for human *PERILIPIN1* and *FABP4* are described in [8].

Microcomputed tomography analysis. Anesthetised animals were introduced in a SkyScan-1178 X-ray tomograph and analysed as previously described [9]. In

brief, mice were scanned using the following parameters: 104 µm voxel size, 49 kV, 0.5 mm thick aluminum filter and a rotation step of 0.9°. Subcutaneous and intra-abdominal adipose tissue volumes were determined in 250 slides of a 20.5 mm segment in the abdominal cavity between the lumbar vertebra 3 (L3) and the caudal vertebra 1 (C1) using NRecon and CTAn softwares (Bruker, Kontich, Belgium).

Adipose tissue histology. Epididymal adipose tissue was collected, fixed for 24 hours in 4% paraformaldehyde, paraffin-embedded and serially cut in 4 µm sections using a microtome HM340E (Leica). Slices were then deparaffinated and stained with hematoxylin and eosin. Micrographs were obtained with a DMD108 digital microscope and automated analysis of adipocytes surface was performed using an in-house ImageJ software macro.

Cell culture. Preparation of stromal vascular fraction (SVF) of epididymal adipose tissue was performed as described in [10]. Briefly, intra-abdominal white epididymal fat depots were collected, washed in PBS, minced then digested for 30 min at 37°C in DMEM supplemented with 2 mg/ml collagenase A (Roche) and 20 mg/ml bovine serum albumin (Sigma-Aldrich). The lysate was successively filtered through 250, 100, and 27 µm nylon meshes and centrifuged for 5 min at 500 g. The pellet containing SVF cells were plated and maintained in DMEM containing 10% FBS until confluence. Differentiation was induced in the same medium supplemented with 1 µM dexamethasone, 0.5 mM

isobutylmethylxanthine, and 340 nM insulin for 2 days. Cells were then maintained for 10 days in the presence of 340 nM insulin for the induction of adipogenesis. hMADS cells were described in [8, 11], transfected with anti-*FMR1 siRNA* (Invitrogen): CCCACCUCCUGUAGGUUAUAAUAAA/UUUAUUAUAACCU ACAGGAGGUGG) or control *siRNA* (Stealth, Invitrogen), using HiPerFect Transfection Reagent (Qiagen) and differentiated into adipocytes as described in [8, 11].

Lipolysis assays. For *in vivo* lipolysis experiments, 6 hours-fasted *Fmr1*-KO and WT were injected intraperitoneally with either saline or isoproterenol at 1 mg/Kg. Fifteen minutes after injection, blood was sampled for glycerol determination in serum. For *ex vivo* lipolysis experiments, 6 hours-fasted *Fmr1*-KO and WT mice were sacrificed, and intra-abdominal white epididymal fat depots were sampled, washed in PBS, then cut in explants of 15-20 mg each, and weighed. Explants were then incubated for 1 hr in DMEM low glucose (1 g/L) supplemented with 15 mM Hepes, 0.5 % bovine serum albumin (Sigma-Aldrich) and then treated with 1 µM isoproterenol or vehicle. A sample of medium was taken for determination of glycerol content at 0, 60, 90, 120, 150 and 180 min after treatment. Glycerol release was then normalized to initial explant mass. Glycerol concentration in serum or medium was determined using Glycerol Free reagent kit (Sigma-Aldrich), according to the manufacturer's instructions. Lipolysis experiments of SVF-derived adipocytes were performed as described in [10], using 1 µM of isoproterenol for 1 hr 30 min. Lipolysis of human hMAD-derived adipocytes was

performed after 10 days of differentiation. Cells were over-night insulin deprived and then submitted to 1µM isoproterenol treatment in fresh media. At indicated times, sampled media were used to measure glycerol and free fatty acid release using Free Glycerol Reagent and Free Fatty Acid Quantification Assay Kit (Abcam) according to the manufacturer's instructions. Concomitantly, cells were lysed with NaOH 0.2N and neutralized with HCl 0.2N. Lysates were used to evaluate triglyceride content using Triglyceride and Free Glycerol reagents (Sigma-Aldrich) and protein content using BCA kit (Sigma-Aldrich) according to the manufacturer's instructions. TG, glycerol and FFA levels were then normalized to protein content in the corresponding well.

Indirect calorimetry. Indirect calorimetry experiments were performed at the Anexplo Genotoul metabolic phenotyping platform (Toulouse, France). 4-mths old male *Fmr1*-KO and WT animals were habituated for 24 hr in indirect calorimetry chambers (Phenomaster System, TSE). Over the following 24 hr, the automated device recorded drink and food consumption, activity monitored by the number of infrared beam breaks, O_2 consumption (VO_2 in $mL/h/kg^{0.75}$) and CO_2 production (VCO_2 in $mL/h/kg^{0.75}$). Energetic expenditure (H_2 in $kcal/h/kg^{0.75}$) and Respiratory Exchange Ratio (RER) were then calculated as described [12].

Proteome analysis. Livers from 4 months-old overnight fasted animals were quickly collected after cervical dislocation, snapped frozen in liquid nitrogen and kept at -80°C until further analysis. Livers were lysed in lysis buffer (25 mM Tris-

HCl pH 7.6, 150 mM NaCl, 1% NP-40, 1% sodium deoxycholate, 0.1% SDS), disrupted with ceramic beads using the FastPrep apparatus (MP Biomedicals) set at Power 6 for 40 s. Lysates were centrifuged at 12,000g, 20 min at 4°C. 100 µL of supernatant were precipitated overnight at -20°C with 900 µL of an acetone:methanol solution (8:1), centrifuged at 2,200g, 20 min at 4°C. Pellet was further rinsed with 80% acetone, then air-dried. The dried protein pellets were resuspended in denaturation buffer (6 M urea, 2 M thiourea in 10 mM Tris, pH 8.5) and quantified using the Bradford assay (Bio-Rad, Munich, Germany). Proteins were digested by in-solution digestion. Briefly, proteins were reduced with 3 mM dithiothreitol, alkylated with 9 mM iodoacetamide, predigested for three hours with 1:100 (w/w) Lys-C (Wako, Germany) and digested with 1:100 (w/w) trypsin (Promega, USA) for 14 hours shaking at room temperature. Before trypsin digestion, samples were diluted with 6 volumes of 50 mM ammonium bicarbonate. Following digestion, samples were acidified with formic acid (FA) to a final concentration of 0.5 % (v/v). Samples were measured on an EASY-nLC 1200 (Thermo Fisher Scientific) coupled to an Orbitrap Elite mass spectrometer (Thermo Fisher Scientific). Peptides were chromatographically separated using 75 µm (ID), 15 cm columns packed in-house with reversed-phase ReproSil-Pur 120 C18-AQ 1.9 µm resin (Dr. Maisch GmbH). Peptides were then eluted using a 169 min non-linear gradient of solvent B (80% ACN, 0.1% formic acid) in the increments; 8 % - 27 % over 142 min, 27 % – 35 % over 24 min and 35 % – 50 % over 3 min. Full-scans were recorded between 300-2000 Thompson at a resolution of 120,000 with a target value of 1E6. The top 15 most intense ions

from each full scan were selected for fragmentation (MS/MS) by higher-energy collisional dissociation (HCD) using a collision energy of 35% at a target value of 5000 charges. Both MS and MS/MS scans were recorded in the orbitrap. All acquired MS data were processed with the MaxQuant software suite [13] version 1.5.2.8 against the complete mouse UniProt database (taxonomy ID 10090) containing 54,506 sequences and a database of 248 frequently observed contaminants. Precursor mass tolerance was set to 6 ppm and 0.5 Da for MS/MS fragment ions. A maximum of two missed cleavages resulting in a minimal length of seven amino acids and full tryptic enzyme specificity were required. Oxidation of methionine and protein N-terminal acetylation were defined as variable modifications and carbamidomethylation of cysteines was used as fixed modification. False discovery rate was set to 1% for peptide and protein identifications. For label-free quantification (LFQ), runs with a 0.7 min matching window were selected. MS proteomics data have been deposited to the ProteomeXchange Consortium via the PRIDE partner repository[14] with the dataset identifier PXD007241 (Username: reviewer52669@ebi.ac.uk; Password: dc4JzXam). Comparison analysis for individual protein levels between genotype was run on normal rank-based inverse log-transformed label-free quantification (LFQ) values and individual FDR were calculated. GO analysis on significantly affected proteins was performed on the subset of proteins with FDR ≤ 0.01 and absolute FC ≥ 1.5 using String (v10.5) [15] and Panther (v12.0) expression analysis tools [16, 17].

Generation of the FL83B cell lines. The FL83B embryonic hepatocytic cell line was ordered to ATCC (CRL-2390) and cultured according to the guidelines in F12K complete medium containing 10% fetal bovine serum. FL83B cells were transduced as described in [18], using a lentivirus expressing either an anti-*Fmr1* shRNA targeting *Fmr1* constitutive exon 1 (*shFmr1*) or a control shRNA (*shControl*). Co-expression of the shRNA is coupled to eGFP expression to enable sorting of transduced cells using a FACS Aria III (BD) based on eGFP fluorescence as described in [18].

Immunofluorescence. FL83B cells were grown subconfluent, fixed in 4% paraformaldehyde and subjected to immunofluorescence labeling using anti-S6 polyclonal rabbit antibodies (Cell signalling) and anti-FMRP Y#C10 polyclonal avian antibodies [19] and secondary antibodies coupled either to AlexA594 or AlexA647, as described in [20]. After counterstaining with DAPI, coverslips were mounted on slides with anti-fading reagent and observed using a Zeiss Axioplan2 epifluorescence microscope equipped with a CoolSNAP HQ CCD cooled camera (Roper Scientific). Micrographs were then analysed with ImageJ software.

Puromycin labeling of neosynthetized peptides. The assay was performed as described in [21]. In brief, FL83B cells were seeded at a density of 100,000 cells/well in 12 well plates. 48 hr post seeding, complete medium was changed for fresh F12K medium. After 5 hr, puromycin was added to the wells at a final concentration of 10 μg/mL. After 15 and 30 min, incorporation of puromycin was

stopped by washing the cells 3 times in ice-cold PBS. Control experiments were perfomed by preincubating cells for 30 min with the translation blocker cycloheximide (50 μg/mL). Cell were scraped in lysis buffer (10 mM Tris pH 7.4, 150mM NaCl, 1.25 mM MgCl2, 0.5% NP40) containing a complete antiprotease cocktail (Pierce). 20 μg of proteins were loaded on a 11% SDS-PAGE and transferred on a nitrocellulose membrane. Ponceau staining was performed to quantify the total protein load in each lane, as described [21, 22]. Puromycin-labeled neosynthetized peptides were visualized by western-blotting using the anti-puromycin 12D10 antibody (Millipore). Signal was visualized using ECL kits (Perkin) and a Fusion VX-Imager (Vilber). Puromycin signal was normalized to total protein Ponceau signal, with both signals quantified in each lane by densitometric analysis using the ImageJ software. Scans of the fully uncut Ponceau-stained membranes as well as anti-puromycin western-blots are available upon request.

Metabolic network reconstruction. The MetaboSignal R package (https://bioconductor.org/packages/release/bioc/html/MetaboSignal.html) was used to build the shortest paths network of relevant proteins and metabolites [23, 24]. An extended list of metabolites (Table S5) was built to recapitulate the classes of metabolites of interest identified using metabolomics or biochemical measurements of circulating markers presented in Figure 1. A network of human pathways was then built merging KEGG, OmniPath and TRRUST databases. A number of interactions were manually implemented (Table S6): interactions for

acetone, L-carnitine, GYS2, AGL, ABCD3, and SLC16A1 were manually curated from the literature [25-30] and proteins significantly dysregulated in the *Fmr1*-KO liver were mapped in the first network of interaction with FMRP. Since human pathways are more complete in those databases, we used human Entrez ID, at the expense of 22 significant mouse proteins with no human homolog that were not considered in the network analysis: *Cyp2a12, Cyp3a25, Cyp2c37, Cyp2c50, Cyp2c67, Cyp2c54, Cyp2j5, Hsd3b5, Slco1a1, Rdh7, Ugt2b7, Chil3, Ugt1a9, Ngp, Cyp2d22, Cyp2a5, Cyp2d26, Gulo, Cyp2c23, Cyp2d10, Cyp2d9, Ighv1-31*. Shortest paths network from FMRP to the metabolites of interest were then computed and visualised in Cytoscape [31]. Finally, the network metric of pivotal betweenness (PB, [32]) was computed for each protein mapped onto the network (Table S7).

Immunoaffinity (IA) capture of FMRP complexes in FL83B cells or liver extracts. Either FL83B cells or *Fmr1*-WT and –KO liver were homogenized in IA buffer (10 mM Tris pH 7.4, 150mM NaCl, 1.25 mM MgCl2, 0.5% NP40, 1mM DTT, 5U/mL RNasin (Invitrogen)). Homogenates were centrifuged at 10,000g for 15 min at 4°C. The supernatant was then raised to 400mM NaCl and 30 mM EDTA and pre-cleared for 1 hr with 60 μL of agarose beads recognizing avian IgY (Gallus) (pre-blocked with 0.1 mg/ml yeast tRNA, and glycogen (Invitrogen)) and with 120 μL of untreated agarose beads (Gallus). Per IA assay, 500 μg of supernatant was incubated in the presence of 60 μg of anti-FMRP Y#C10 antibodies or unrelated IgY (Gallus) immobilized on 15 μL of agarose beads. Samples were

incubated overnight rotating at 4°C and washed 4 times with IA wash buffer (10 mM Tris pH 7.4, 400mM NaCl, 10 mM EDTA, 0.5% NP40). 1/5th of each assay was used for protein analysis using anti-FMRP mAb1C3 antibody [33] and the remaining was subjected to DNAase I treatment (Ambion) for 15 min on ice followed by proteinase K treatment (Roche) for 15 min at RT. IA-captured mRNAs were then phenol-extracted, precipitated with sodium acetate and resuspended in water. The integrity of RNAs extracted from the input and the flowthrough post-IA supernatant was verified on a 1.5% agarose gel. RNA from input lysates and IA assays were subjected to reverse transcription (RT) using the SuperScript III system (Invitrogen), according to the manufacturer's instructions. RT products were subjected to polymerase chain reaction (PCR), using a PCR Master Kit (Promega). Primers used and amplicons lengths are listed in Table S9. The PCR program consisted in 10 min of initial denaturation at 95°C followed by 28 to 35 cycles consisting of 30 s at 95°C, 15 s at 58°C, 15 s at 72°C, and a final elongation step of 10 min at 72°C. PCR products were visualised on a 2.5% TAE agarose gel and amplicon size was verified using the BenchTop DNA ladder (Promega). Primers used are detailed in Table S8.

Clinical samples. Twenty-nine healthy subjects (24 males, 5 females) and 25 fragile X patients (20 males, 5 females) of matching ages and ethnicity were enrolled at the University of Antwerp (Antwerp, Belgium). The absence/presence of the Fragile X full mutation in the 5' UTR of *FMR1* gene was confirmed in all participants by an accredited laboratory, using a CGG-repeat PCR and Southern

Blotting on DNA isolated from blood. All patients were between 6-18 years of age and had a number of CGG repeats above 200 yielding *FMR1* gene inactivation (Pieretti et al., 1991). Informed consent was obtained from each participant or his legal guardian before research participation. For this study, we privileged unmedicated patients or under stable treatment for the past 8 wks. Patients under anti-psychotic treatment were systematically excluded. Out of the 25 patients involved, 3 were under Ritaline treatment and were advised not to take the drug on the day of sampling. Exclusion criteria were: recent history of seizure, epilepsy, or blackouts, clinically unstable medical disease, progressive CNS disease/disorder, history of psychiatric disorders, behavioural dysfunction to the point that subject cannot cooperate for testing and history of pathologies which could modify blood biochemistry (*e.g.* diabetes). To avoid stress induced by fasting to Fragile X patients, individuals involved in the study were not advised to fast prior sampling. Blood was withdrawn in serum collection tubes (BD Vacutainer Serum Separator Tubes), incubated for at least 30 min at room temperature then centrifuged at 2000 rpm, 10 min, at room temperature. Serum was collected, aliquoted and immediately snapped-frozen in liquid nitrogen prior storage at -80°C until use.

Measures in human samples. ^{1}H-NMR metabolic profiling of nonfasting sera samples from FXS patients and controls was performed as described for murine samples. The determination of circulating FFA was subcontracted to the Genotoul Anexplo Platform (Toulouse, France). Insulin was measured using an

Electro-Chemo-Luminescence (ECL)-based assay (v-plex®, MesoScaleDiscovery).

Statistics. Normality of data was assessed using Kolmogorov-Smirnov's test. To compare 2 groups, 2-tailed unpaired Student's T-test was used. For non-normal data, log-transformation was applied to meet normality criteria prior to Student's T-test. If sample size n<8 or if normality was not reached after log-transformation, data were analyzed using Mann & Whitney's non-parametrical U-test. Multiple group comparisons were performed using two-way ANOVA with Genotype (or *siRNA* or *shRNA*) and Treatment or Time as factors or using three-way ANOVA with Genotype, Treatment and Time as factors as stated in legends and text. *Post hoc* comparisons were performed either using Šidák's correction for multiple comparison or Fisher's Least Significance Difference test (if less than 6 comparisons were performed), as stated in the legends. The details of ANOVA statistics are presented in Table S9. Statistical significance was set according to a two-tailed pvalue (p)<0.05. Only significant differences are displayed on the graphs. Statistical analysis was performed using GraphPad Prism version 6.00 for iOS (GraphPad Software, USA).

Study approvals. All animal studies were conducted in facilities accredited by legal authorities (Direction Départementale de Protection des Populations des Alpes-Maritimes, accreditation #C-06-152-5). Procedures involving animal experimentation were approved by the local animal experimentation ethics

committee (Comité Institutionnel d‘Éthique Pour l‘Animal de Laboratoire) and registered at the Ministère de l'Enseignement Supérieur et de la Recherche (agreement #00788.01 and #05224.01). Samples and data collection from Fragile X patients and controls was approved by the medical ethics committee of the University of Antwerp in Belgium (agreement #B300201523589). The study was conducted in accordance with statutes and regulations regarding the protection of the right and welfare of human subjects’ participation in biomedical research (World Declaration of Helsinki).

Supplemental figures

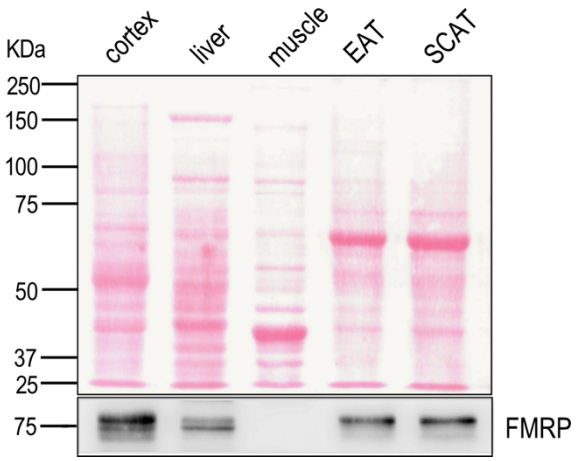

Figure S1. Expression of FMRP in various tissues.

Ponceau staining of membrane and Western-blot using anti-FMRP mAb1C3 monocolanl antibody in cortex, liver, muscle (quadriceps), epididymal (EAT) and sub-cutaneous (SCAT) adipose tissues of a 4-months old WT mouse. Note the expression of FMRP in the cortex, liver and both adipose tissues (EAT and SCAT) and the lack of expression in muscle in agreement with [34], supporting the specificity of the staining.

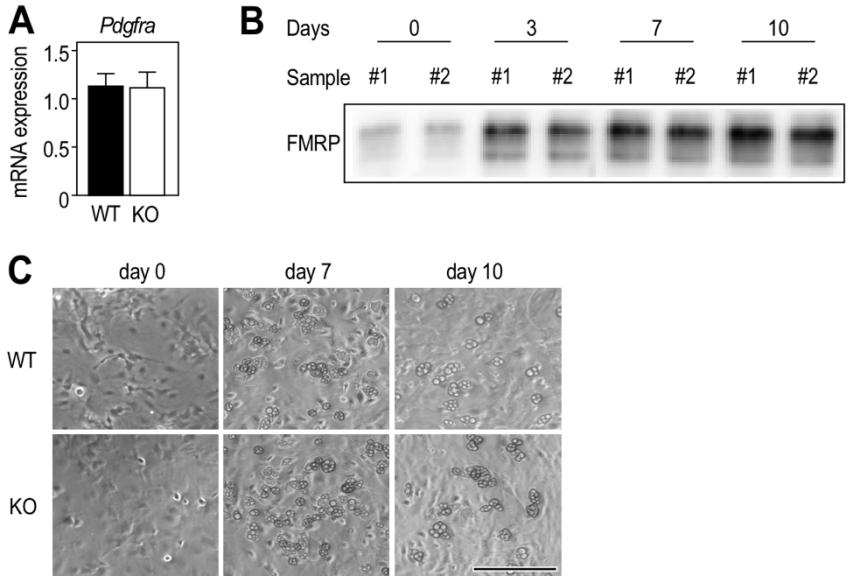

Figure S2. *Fmr1*-deficiency does not affect adipocytes differentiation

(A) mRNA levels of adipocyte progenitor marker *Pdgfra* in *Fmr1*-WT and -KO WAT. Data are means ± SEM of mRNA level relative to WT; n=8 WT, n=9 KO. 2-tailed Student's T-test: ns.

(B) Western-blot analysis of FMRP expression in cells derived from two independent preparations (#1 and #2) of epididymal adipose tissue-derived stromal vascular fraction (SVF) cells at 0, 3, 7 and 10 days of differentiation into adipocytes. 15μg of proteins were loaded in each lane.

(C) Microphotographs showing the course of differentiation of SVF derived adipocytes from *Fmr1*-KO and WT WAT. Black bar represents 200 μm.

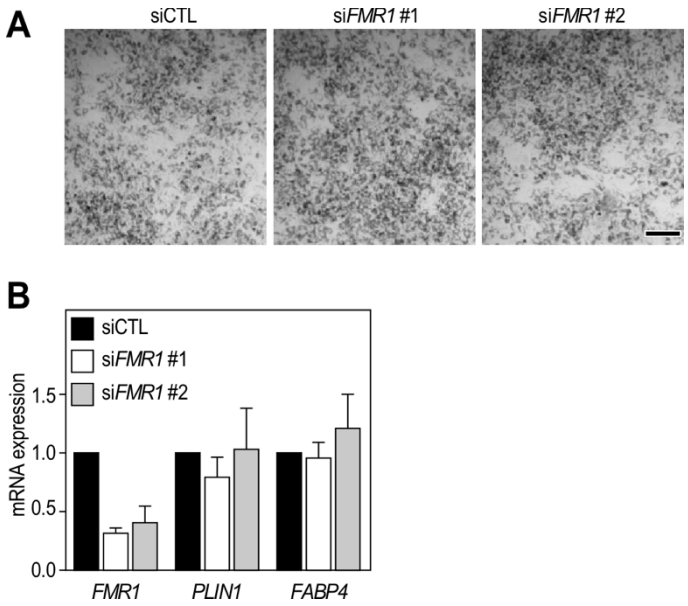

Figure S3. *Fmr1*-deficiency does not affect hMADs differentiation into adipocytes.

(A) Microphotographs of hMADs-derived adipocytes transfected with a silencing RNA targeting *FMR1* transcript constitutive exon (*siFMR1*) or a control (*siCtl*) siRNA. Black bar represents 200 µm.

(B) Quantitative RT-PCR determination of *FMR1, PLIN1* and *FABP4* mRNA expression in hMADs-derived adipocytes transfected with si*FMR1* or *siCtl*. Data are means ± SEM relative to *siCtl*; n=4/condition; 2-way ANOVA: p(siRNA)=0.001, p(Transcript)=0.0144, p(Interaction)=0.0144; Šidák's post hoc tests: ***, p<0.001.

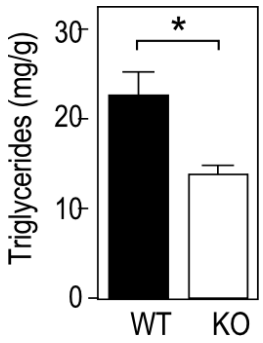

Figure S4. *Fmr1*-deficiency reduces hepatic TG content. Data are means TG levels per gram of tissue ± SEM; n=9 WT, n=9 KO; 2-tailed Student's T-test: *, $p<0.05$.

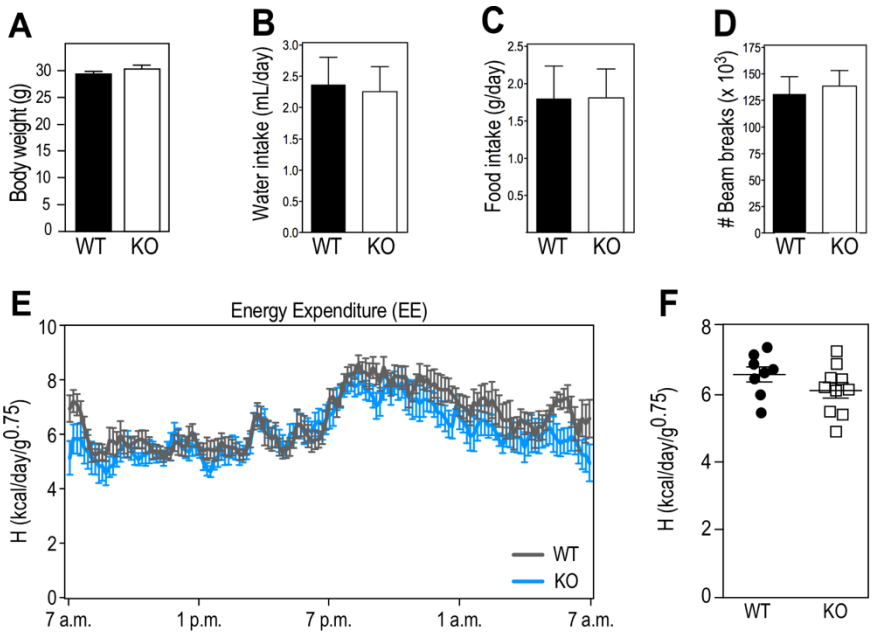

Figure S5. *Fmr1*-deficiency does not modify body weight, water intake, food intake, locomotor activity or energetic expenditure.

(A) Body weight in 4-mths old *Fmr1*-KO and WT littermates. Data are means ± SEM; n=8 WT, n=10 KO; 2-tailed Student's T-test: ns.

(B) Drinking water intake over 24 hrs. Data are means ± SEM; n=8 WT, n=10 KO; 2-tailed Student's T-test: ns.

C) Food intake over 24 hrs. Data are means ± SEM; n=8 WT, n=10 KO; 2-tailed Student's T-test: ns.

(D) Total activity measured by the number of infrared beam breaks over 24 hrs. Data are means ± SEM; n=8 WT, n=10 KO; 2-tailed Student's T-test: ns.

(E) Energy expenditure follow-up by over 24 hrs (10 min bin). n=8 WT, n=10 KO.

(F) Average EE over 24 hrs. Data are means ± SEM; n=8 WT, n=10 KO; 2-tailed Student's T-test: ns.

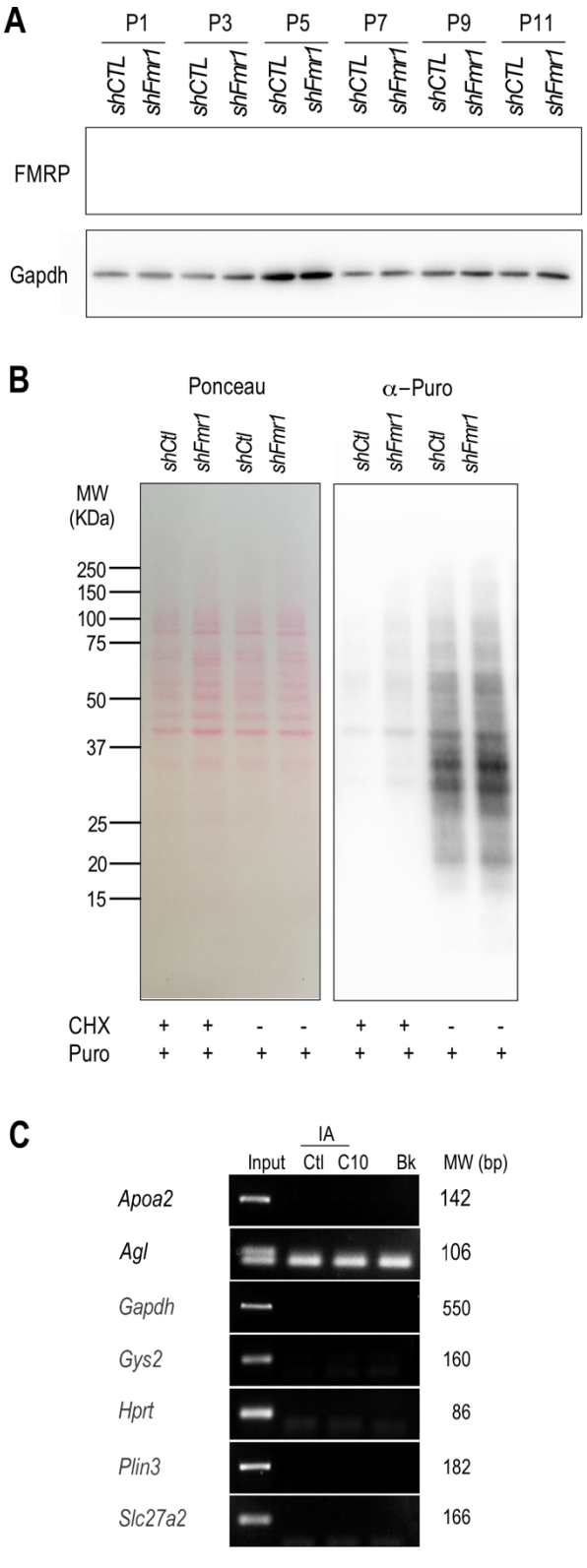

Figure S6. Controls for *Fmr1* repression, Sunset and IA experiments in the FL83B hepatocytic cell line.

(A) FL83B cells transduced with *shFmr1* show stable depletion of FMRP over passages as compared to *shCtl*-transduced cells. Western-blot using anti-FMRP mAb1C3 antibody in shControl (*shCtl*) and *shFmr1* cell lines at different passages (P). Gapdh was used as a loading control. 15 μg of proteins were loaded per lane.

(B) Anti-puromycin antibody selectively label neosynthetized peptides in *shFmr1* and *shCtl* FL83B cell lines. Cells were pretreated with the translation inhibitor cycloheximide (CHX) for 30 min or with vehicle as indicated and then labelled with puromycin (puro) for 30 min. Cell homogenates were analyzed by Ponceau or western blot with anti-puromycin antibody (α-Puro). Note the strong reduction in puromycin signal in the presence of CHX. 15 μg of proteins were loaded per lane.

(C) RT-PCR analysis of mRNAs associated with FMRP in FL83B hepatocytes. Total RNA was extracted from the input cell lysate and IA preparations described in (Figure 6B), and used as a template for RT-PCR. PCR products obtained from input, control IgY (IA Ctl) or IgY#C10 (IA C10) IA complexes as well as control blank PCR (Ctl) performed in the absence of matrix were separated and visualized by agarose gel electrophoresis. PCR amplicons lengths (bp) are specified on the right side. (*) Amplicon likely to correspond to aspecific primer dimers amplification. The *Agl* specific band is the upper one only detected in the Input.

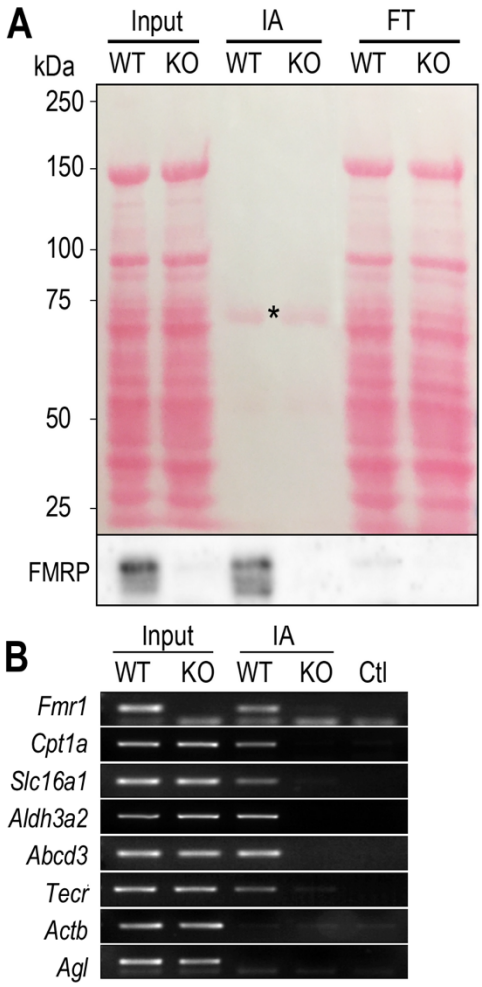

Figure S7. FMRP associates with selective mRNAs in the liver

(A) Liver homogenates from *Fmr1*-WT and KO fasted mice were subjected to immuno-affinity (IA) capture with anti-FMRP IgY#C10 avian antibodies and the eluted proteins as well as the post-IA flowthrough supernatant (FT) were analyzed by immunoblotting using anti-FMRP mAb1C3. IgY heavy chains are labeled with an asterisk on the Ponceau (upper panel). Note that depletion in FMRP load in the post-immunoprecipitation supernatant in the presence of IgY#C10 as compared to *Fmr1*-WT input.

(B) RT-PCR analysis of mRNAs associated with FMRP in the liver. Total RNA was extracted from the input *Fmr1*-WT and KO liver lysates and FMRP IA-captured complexes and used as a template for RT-PCR. RT-PCR products obtained from input *Fmr1*-WT or KO liver (lanes 1, 2) and IgY#C10 IA preparations from *Fmr1*-WT or KO liver (lanes 3, 4), as well as control PCR (lane 5) performed in the absence of matrix were separated and visualized by agarose gel electrophoresis. This reveals that the known FMRP mRNA target *Fmr1* is selectively recovered in the IgY#C10 IA-captured complexes from *Fmr1*-WT liver. The mRNAs *Cpt1a, Slc16a1, Aldh3a2, Abcd3, Tecr* are also selectively recovered in the IgY#C10 immunoprecipitate, while the mRNA *Actb and Agl* were not recovered. The molecular weights of PCR amplicons are specified on the right side.

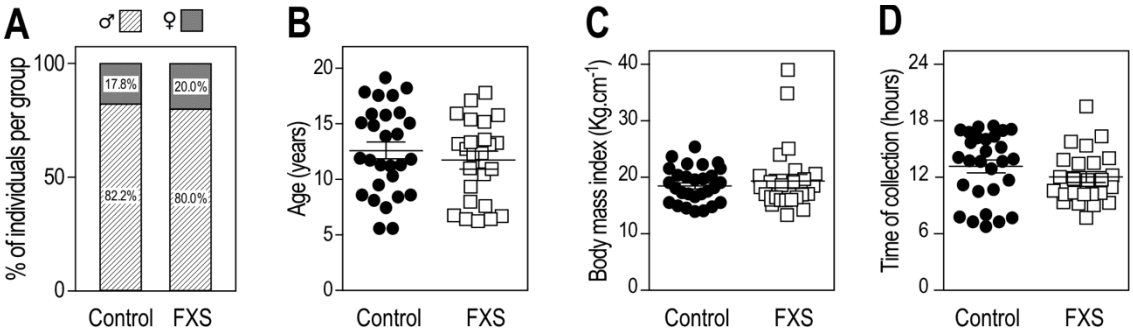

Figure S8. Characteristics of the FXS and control individuals involved in the clinical study.

(A) Sex distribution; n=29 controls and n=25 FXS patients; Chi-square test: ns.

(B) Age distribution. Data are means ± SEM; n=29 controls and n=25 FXS patients; 2-tailed Student's T-test: ns.

(C) Body mass index distribution. Data are means ± SEM; n=29 controls and n=25 FXS patients; 2-tailed Mann & Whitney U-test: ns.

(D) Distribution of sample collection's time. Data are means ± SEM; n=29 controls and n=25 FXS patients; 2-tailed Mann & Whitney U-test: ns.

Supplementary tables legends

Table S1. Individual LFQ scores for the samples used in proteome analysis.

Available as Excel file

Table S2. List of 307 proteins showing a significant change in abundance of at least 1.5-fold (FDR ≤ 0.01) in *Fmr1*-deficient fasted liver as compared to control.

Available as Excel file

Table S3. String-based Gene Ontology analysis of pathways significantly overrepresented in list of 307 of proteins showing a significant change (FDR ≤ 0.01) and absolute fold-of-chance in abundance of at least 1.5 in *Fmr1*-deficient fasted liver as compared to control.

Available as Excel file

Table S4. Panther-based Gene Ontology analysis of pathways significantly overrepresented in list of 307 of proteins showing a significant change (FDR ≤ 0.01) and absolute fold-of-chance in abundance of at least 1.5 in *Fmr1*-deficient fasted liver as compared to control.

Available as Excel file

Table S5. Metabolic network extended metabolite list.

Available as Excel file

Table S6. Metabolic network extended node list. Gene (EntrezGene ID) or metabolite (KEGG ID), reference for interaction

Available as Excel file

Table S7. Metabolic network metrics. Human Entrez Gene IDs, Gene name, Protein name and normalized pivotal betweenness (PB) score for proteins mapped on the network.

Available as Excel file

Table S8. List of primers.

Available as Excel file

Table S9. ANOVA statistics.

Available as Excel file

References

[1] Mientjes, E.J., Nieuwenhuizen, I., Kirkpatrick, L., Zu, T., Hoogeveen-Westerveld, M., Severijnen, L., et al., 2006. The generation of a conditional Fmr1 knock out mouse model to study Fmrp function in vivo. Neurobiol Dis 21(3):549-555.

[2] Dona, A.C., Jimenez, B., Schafer, H., Humpfer, E., Spraul, M., Lewis, M.R., et al., 2014. Precision high-throughput proton NMR spectroscopy of human urine, serum, and plasma for large-scale metabolic phenotyping. Anal Chem 86(19):9887-9894.

[3] Dona, A.C., Kyriakides, M., Scott, F., Shephard, E.A., Varshavi, D., Veselkov, K., et al., 2016. A guide to the identification of metabolites in NMR-based metabonomics/metabolomics experiments. Comput Struct Biotechnol J 14:135-153.

[4] Dumas, M.E., Barton, R.H., Toye, A., Cloarec, O., Blancher, C., Rothwell, A., et al., 2006. Metabolic profiling reveals a contribution of gut microbiota to fatty liver phenotype in insulin-resistant mice. Proc Natl Acad Sci U S A 103(33):12511-12516.

[5] Heikkinen, S., Argmann, C.A., Champy, M.F., Auwerx, J., 2007. Evaluation of glucose homeostasis. Curr Protoc Mol Biol Chapter 29:Unit 29B 23.

[6] Ayala, J.E., Samuel, V.T., Morton, G.J., Obici, S., Croniger, C.M., Shulman, G.I., et al., 2010. Standard operating procedures for describing and performing metabolic tests of glucose homeostasis in mice. Dis Model Mech 3(9-10):525-534.

[7] Livak, K.J., Schmittgen, T.D., 2001. Analysis of relative gene expression data using real-time quantitative PCR and the 2(-Delta Delta C(T)) Method. Methods 25(4):402-408.

[8] Rodriguez, A.M., Elabd, C., Delteil, F., Astier, J., Vernochet, C., Saint-Marc, P., et al., 2004. Adipocyte differentiation of multipotent cells established from human adipose tissue. Biochemical and biophysical research communications 315(2):255-263.

[9] Beranger, G.E., Pisani, D.F., Castel, J., Djedaini, M., Battaglia, S., Amiaud, J., et al., 2014. Oxytocin reverses ovariectomy-induced osteopenia and body fat gain. Endocrinology 155(4):1340-1352.

[10] Pisani, D.F., Beranger, G.E., Corinus, A., Giroud, M., Ghandour, R.A., Altirriba, J., et al., 2016. The K+ channel TASK1 modulates beta-adrenergic response in brown adipose tissue through the mineralocorticoid receptor pathway. FASEB J 30(2):909-922.

[11] Pisani, D.F., Djedaini, M., Beranger, G.E., Elabd, C., Scheideler, M., Ailhaud, G., et al., 2011. Differentiation of Human Adipose-Derived Stem Cells into "Brite" (Brown-in-White) Adipocytes. Front Endocrinol (Lausanne) 2:87.

[12] Even, P.C., Nadkarni, N.A., 2012. Indirect calorimetry in laboratory mice and rats: principles, practical considerations, interpretation and perspectives. Am J Physiol Regul Integr Comp Physiol 303(5):R459-476.

[13] Cox, J., Mann, M., 2008. MaxQuant enables high peptide identification rates, individualized p.p.b.-range mass accuracies and proteome-wide protein quantification. Nat Biotechnol 26(12):1367-1372.

[14] Vizcaino, J.A., Csordas, A., Del-Toro, N., Dianes, J.A., Griss, J., Lavidas, I., et al., 2016. 2016 update of the PRIDE database and its related tools. Nucleic Acids Res 44(22):11033.

[15] Jensen, L.J., Kuhn, M., Stark, M., Chaffron, S., Creevey, C., Muller, J., et al., 2009. STRING 8--a global view on proteins and their functional interactions in 630 organisms. Nucleic Acids Res 37(Database issue):D412-416.

[16] Thomas, P.D., Campbell, M.J., Kejariwal, A., Mi, H., Karlak, B., Daverman, R., et al., 2003. PANTHER: a library of protein families and subfamilies indexed by function. Genome Res 13(9):2129-2141.

[17] Thomas, P.D., Kejariwal, A., Guo, N., Mi, H., Campbell, M.J., Muruganujan, A., et al., 2006. Applications for protein sequence-function evolution data: mRNA/protein

expression analysis and coding SNP scoring tools. Nucleic Acids Res 34(Web Server issue):W645-650.

[18] Khalfallah, O., Jarjat, M., Davidovic, L., Nottet, N., Cestele, S., Mantegazza, M., et al., 2017. Depletion of the Fragile X Mental Retardation Protein in Embryonic Stem Cells Alters the Kinetics of Neurogenesis. Stem Cells 35(2):374-385.

[19] El Fatimy, R., Tremblay, S., Dury, A.Y., Solomon, S., De Koninck, P., Schrader, J.W., et al., 2012. Fragile X mental retardation protein interacts with the RNA-binding protein Caprin1 in neuronal RiboNucleoProtein complexes [corrected]. PLoS ONE 7(6):e39338.

[20] Dury, A.Y., El Fatimy, R., Tremblay, S., Rose, T.M., Cote, J., De Koninck, P., et al., 2013. Nuclear Fragile X Mental Retardation Protein is localized to Cajal bodies. PLoS genetics 9(10):e1003890.

[21] Schmidt, E.K., Clavarino, G., Ceppi, M., Pierre, P., 2009. SUnSET, a nonradioactive method to monitor protein synthesis. Nat Methods 6(4):275-277.

[22] Gantois, I., Khoutorsky, A., Popic, J., Aguilar-Valles, A., Freemantle, E., Cao, R., et al., 2017. Metformin ameliorates core deficits in a mouse model of fragile X syndrome. Nat Med 23(6):674-677.

[23] Rodriguez-Martinez, A., Ayala, R., Posma, J.M., Dumas, M.E., 2018. Exploring the Genetic Landscape of Metabolic Phenotypes with MetaboSignal. Curr Protoc Bioinformatics 61(1):14 14 11-14 14 13.

[24] Rodriguez-Martinez, A., Ayala, R., Posma, J.M., Neves, A.L., Gauguier, D., Nicholson, J.K., et al., 2017. MetaboSignal: a network-based approach for topological analysis of metabotype regulation via metabolic and signaling pathways. Bioinformatics 33(5):773-775.

[25] Koorevaar, G., Van Stekelenburg, G.J., 1976. Mammalian acetoacetate decarboxylase activity. Its distribution in subfractions of human albumin and occurrence in various tissues of the rat. Clin Chim Acta 71(2):173-183.

[26] Miyazawa, S., Ozasa, H., Osumi, T., Hashimoto, T., 1983. Purification and properties of carnitine octanoyltransferase and carnitine palmitoyltransferase from rat liver. J Biochem 94(2):529-542.

[27] Algranati, I.D., Cabib, E., 1960. The synthesis of glycogen in yeast. Biochim Biophys Acta 43:141-142.

[28] Whelan, W.J., 1971. Enzymic explorations of the structures of starch and glycogen. Biochem J 122(5):609-622.

[29] Imanaka, T., Aihara, K., Takano, T., Yamashita, A., Sato, R., Suzuki, Y., et al., 1999. Characterization of the 70-kDa peroxisomal membrane protein, an ATP binding cassette transporter. J Biol Chem 274(17):11968-11976.

[30] Halestrap, A.P., 2013. The SLC16 gene family - structure, role and regulation in health and disease. Mol Aspects Med 34(2-3):337-349.

[31] Shannon, P., Markiel, A., Ozier, O., Baliga, N.S., Wang, J.T., Ramage, D., et al., 2003. Cytoscape: a software environment for integrated models of biomolecular interaction networks. Genome Res 13(11):2498-2504.

[32] Davidovic, L., Navratil, V., Bonaccorso, C.M., Catania, M.V., Bardoni, B., Dumas, M.E., 2011. A metabolomic and systems biology perspective on the brain of the Fragile X syndrome mouse model. Genome Res 12:2190-2202.

[33] Devys, D., Lutz, Y., Rouyer, N., Bellocq, J.P., Mandel, J.L., 1993. The FMR-1 protein is cytoplasmic, most abundant in neurons and appears normal in carriers of a fragile X premutation. Nat Genet 4(4):335-340.

[34] Khandjian, E.W., Bardoni, B., Corbin, F., Sittler, A., Giroux, S., Heitz, D., et al., 1998. Novel isoforms of the fragile X related protein FXR1P are expressed during myogenesis. Hum Mol Genet 7(13):2121-2128.